1

2

3

4

5

6

7 **On the observational determination of climate sensitivity and its implications**

8

9 Richard S. Lindzen[1], and Yong-Sang Choi[2*]

10

11 [1]Program in Atmospheres, Oceans, and Climate, Massachusetts Institute of Technology, Cambridge,

12 MA 02139 USA

13 [2]Department of Environmental Science and Engineering, Ewha Womans University,

14 Seoul, 120-750 Korea

15

16

17

21

22

23 *Corresponding author: Prof. Yong-Sang Choi, E-mail: ysc@ewha.ac.kr.

24

Abstract

We estimate climate sensitivity from observations, using the deseasonalized fluctuations in sea surface temperatures (SSTs) and the concurrent fluctuations in the top-of-atmosphere (TOA) outgoing radiation from the ERBE (1985-1999) and CERES (2000-2008) satellite instruments. Distinct periods of warming and cooling in the SSTs were used to evaluate feedbacks. An earlier study (Lindzen RS, Choi Y-S (2009) *Geophys. Res. Lett.* 36:L16705) was subject to significant criticisms. The present paper is an expansion of the earlier paper where the various criticisms are taken into account. The present analysis accounts for the 72 day precession period for the ERBE satellite in a more appropriate manner than in the earlier paper. We develop a method to distinguish noise in the outgoing radiation as well as radiation changes that are forcing SST changes from those radiation changes that constitute feedbacks to changes in SST. We demonstrate that our new method does moderately well in distinguishing positive from negative feedbacks and in quantifying negative feedbacks. In contrast, we show that simple regression methods used by several existing papers generally exaggerate positive feedbacks and even show positive feedbacks when actual feedbacks are negative. We argue that feedbacks are largely concentrated in the tropics, and the tropical feedbacks can be adjusted to account for their impact on the globe as a whole. Indeed, we show that including all CERES data (not just from the tropics) leads to results similar to what are obtained for the tropics alone – though with more noise. We again find that the outgoing radiation resulting from SST fluctuations exceeds the zero-feedback response thus implying negative feedback. In contrast to this, the calculated TOA outgoing radiation fluxes from 11 atmospheric models forced by the observed SST are less than the zero-feedback response, consistent with the positive feedbacks that characterize these models. The results imply that the models are exaggerating climate sensitivity.

1. Introduction

The heart of the global warming issue is so-called greenhouse warming. This refers to the fact that the earth balances the heat received from the sun (mostly in the visible spectrum) by radiating in the infrared portion of the spectrum back to space. Gases that are relatively transparent to visible light but strongly absorbent in the infrared (greenhouse gases) interfere with the cooling of the planet, forcing it to become warmer in order to emit sufficient infrared radiation to balance the net incoming sunlight (Lindzen, 1999). By net incoming sunlight, we mean that portion of the sun's radiation that is not reflected back to space by clouds, aerosols and the earth's surface. CO_2, a relatively minor greenhouse gas, has increased significantly since the beginning of the industrial age from about 280 ppmv to about 390 ppmv, presumably due mostly to man's emissions. This is the focus of current concerns. However, warming from a doubling of CO_2 would only be about 1°C (based on simple calculations where the radiation altitude and the Planck temperature depend on wavelength in accordance with the attenuation coefficients of well-mixed CO_2 molecules; a doubling of any concentration in ppmv produces the same warming because of the logarithmic dependence of CO_2's absorption on the amount of CO_2) (IPCC, 2007).

This modest warming is much less than current climate models suggest for a doubling of CO_2. Models predict warming of from 1.5°C to 5°C and even more for a doubling of CO_2. Model predictions depend on the 'feedback' within models from the more important greenhouse substances, water vapor and clouds. Within all current climate models, water vapor increases with increasing temperature so as to further inhibit infrared cooling. Clouds also change so that their visible reflectivity decreases, causing increased solar absorption and warming of the earth.

Cloud feedbacks are still considered to be highly uncertain (IPCC, 2007), but the fact that these feedbacks are strongly positive in most models is considered to be an indication that the result is basically correct. Methodologically, this is unsatisfactory. Ideally, one would seek an observational test of the issue. Here we suggest that it may be possible to test the issue with existing data from

73   satellites.

74   Indeed, an earlier study by Forster and Gregory (2006) examined the anomaly of the annual mean

75   temperature and radiative flux observed from a satellite. However, with the annual time scale, the

76   signal of short-term feedback associated with water vapor and clouds can be contaminated by

77   unknown time-varying radiative forcing in nature, and the feedbacks cannot be accurately diagnosed

78   (Spencer, 2010). Moreover, as we will show later in this paper, the regression approach, itself, is an

79   important source of bias. In a recent paper (Lindzen and Choi, 2009) we attempted to resolve these

80   issues though, as has been noted in subsequent papers, the details of that paper were, in important

81   ways, also incorrect (Trenberth *et al*., 2010; Chung et al., 2010; Murphy, 2010). There were four

82   major criticisms to Lindzen and Choi (2009): (i) incorrect computation of climate sensitivity, (ii)

83   statistical insignificance of the results, (iii) misinterpretation of air-sea interaction in the Tropics, (iv)

84   misuse of uncoupled atmospheric models. The present paper responds to the criticism, and corrects

85   the earlier approach where appropriate. The earlier results are not significantly altered, and we show

86   why these results differ from what others like Trenberth *et al*. (2010), and Dessler (2010) obtain.

87

88   **2. Feedback formalism**

89   In the absence of feedbacks, the behavior of the climate system can be described by Fig. 1a. ΔQ is

90   the radiative forcing, G_0 is the zero-feedback response function of the climate system, and ΔT_0 is the

91   response of the climate system in the absence of feedbacks. The checkered circle is a node. Fig. 1a

92   symbolically shows the temperature increment, ΔT_0, that a forcing increment, ΔQ, would produce

93   with no feedback,

94                    $$\Delta T_0 = G_0 \Delta Q \qquad\qquad\qquad (1)$$

95   It is generally accepted that in the absence of feedback, a doubling of CO_2 will cause a forcing of

96   $\Delta Q \approx 3.7 \text{ Wm}^{-2}$ and will increase the temperature by $\Delta T_0 \approx 1.1$ K (Hartmann, 1994; Schwartz,

97 2007). We therefore take the zero-feedback response function of Eq. (1) to be $G_0 \approx 0.3$ (=1.1/3.7) K

98 W^{-1} m^2 for the earth as a whole.

99   With feedback, Fig. 1a is modified to Fig. 1b. The response is now

100 $$\Delta T = G_0(\Delta Q + F\Delta T) \qquad\qquad (2)$$

101   Here F is a feedback function that represents all changes in the climate system (for example,

102 changes in cloud cover and humidity) that act to increase or decrease feedback-free effects. Thus, F

103 should not include the zero-feedback (ZFB) response to ΔT that is already incorporated into G_0. The

104 choice of ZFB response for the tropics in Lindzen and Choi (2009) is certainly incorrect in this

105 respect (Trenberth *et al*., 2010; Chung *et al*., 2010). At present, the best choice seems to remain $1/G_0$

106 (3.3 W m^{-2} K^{-1}) (Colman, 2003; Schwartz, 2007).

107   Solving Eq. (2) for the temperature increment ΔT and inserting Eq. (1) into Eq. (2) we find

108 $$\Delta T = \frac{\Delta T_0}{1 - f} \qquad\qquad (3)$$

109 The dimensionless feedback factor is $f = F\,G_0$. Also, dividing Eq. (2) by G_0, we obtain

110 $$-\frac{f}{G_0}\Delta T = \Delta Q - \frac{\Delta T}{G_0} \qquad\qquad (4)$$

111   When looking at the observations, ΔQ and ΔT in Eq. (4) may be replaced by the change in

112 outgoing net radiative flux, ΔFlux, and the change in sea surface temperature, ΔSST, respectively,

113 leading to

114 $$-\frac{f}{G_0}\Delta \text{SST} = \Delta \text{Flux} - \text{ZFB} \qquad\qquad (5)$$

115 where ZFB indicates the zero-feedback response to ΔSST, i.e., ΔSST$/G_0$. The quantities on the right

116 side of the equation indicate the amount by which feedbacks supplement ZFB response to ΔFlux. At

117 this point, it is crucial to recognize that our equations are predicated on the assumption that the ΔSST

118 to which the feedbacks are responding is produced by ΔFlux. Physically, however, we expect that

119   any fluctuation in temperature should elicit the same flux regardless of the origin of temperature

120   change. Note that the natural forcing, ΔSST, that can be observed, is actually not the same as the

121   equilibrium response temperature ΔT in Eq. (4). The latter cannot be observed since, for the short

122   intervals considered, the system cannot be in equilibrium, and over the longer periods needed for

123   equilibration of the whole climate system, ΔFlux at the top of the atmosphere (TOA) is restored to

124   zero. The choice of the short intervals may serve to remove some natural time-varying radiative

125   forcing that contaminates the feedback signal (Spencer and Braswell, 2010). As explained in Lindzen

126   and Choi (2009), it is essential, that the time intervals considered, be short compared to the time it

127   takes for the system to equilibrate, while long compared to the time scale on which the feedback

128   processes operate (which, in the tropics, are essentially the time scales associated with

129   cumulonimbus convection). The latter is on the order of days, while the former depends on the

130   climate sensitivity, and ranges from years for sensitivities on the order of 0.5°C for a doubling of

131   CO_2 to many decades for higher sensitivities (Lindzen and Giannitsis, 1998).

132   The domain of the data is a major issue with critics. Recent papers (Trenberth *et al.*, 2010; Murphy,

133   2010) argued that quantification of global feedback based on Eq. (5) is inadequate with our tropical

134   domain (20°S–20°N). The argument makes sense since there is the exchange of energy between the

135   tropics and the extratropics. To resolve this issue, modification of Eq. (5) is necessary. Allowing the

136   tropical domain to be an open system that exchanges energy with the rest of the earth, Eq. (5) must

137   be replaced by

138    $$cf \approx -G_0 \left(\frac{\Delta \text{Flux} - \text{ZFB}}{\Delta \text{SST}} \right)_{tropics} \qquad (6)$$

139   where the factor c results from the sharing of the tropical feedbacks over the globe, following the

140   methodology of Lindzen, Chou and Hou (2001), (hereafter LCH01) and Lindzen, Hou and Farrell

141   (1982), The methodology developed in LCH01 permits the easy evaluation of the contribution of

142   tropical processes to the global value. As noted by LCH01, this does not preclude there being

143   extratropical contributions as well. In fact, with the global data (available for a limited period only),

144   the factor c is estimated to be close to unity, so that Eq. (6) is similar to Eq. (5); based on the

145   independent analysis with the global data (Choi *et al.*, 2011) (results from which will be presented

146   later in this paper), it is clear that the use of the global data essentially leads to similar results to that

147   from the tropical data. This similarity is probably due to the concentration of water vapor in the

148   tropics (more details are given in Section 6). With the tropical data in this study, the factor c is

149   simply set to 2; that is to say that the contribution of the tropical feedback to the global feedback is

150   only about half of the tropical feedback. However, we also tested various c values 1.5 to 3 (viz

151   Section 6); as we will show, the precise choice of this factor c does not affect the major conclusions

152   of this study.

153   From Eq. (6), the longwave (LW) and shortwave (SW) contributions to f are given by

154
$$f_{LW} = -\frac{G_0}{c}\left(\frac{\Delta \text{OLR} - \text{ZFB}}{\Delta \text{SST}}\right)_{tropics} \tag{7a}$$

155
$$f_{SW} = -\frac{G_0}{c}\left(\frac{\Delta \text{SWR}}{\Delta \text{SST}}\right)_{tropics} \tag{7b}$$

156   Here we can identify ΔFlux as the change in outgoing longwave radiation (OLR) and shortwave

157   radiation (SWR) measured by satellites associated with the measured ΔSST. Since we know the

158   value of G_0, the experimentally determined slope (the quantity on the right side of Eq. (7)) allows us

159   to evaluate the magnitude and sign of the feedback factor f provided that we also know the value of

160   the ZFB response (ΔSST$/G_0$ in this study). For observed variations, the changes in radiation

161   (associated for example with volcanoes or non-feedback changes in clouds) can cause changes in

162   SST as well as respond to changes in SST, and there is a need to distinguish these two possibilities.

163   This is less of an issue with model results from AMIP (Atmospheric Model Intercomparison Project)

164   where observed variations in SST are specified. Of course, there is always the problem of noise

165   arising from the fact that clouds depend on factors other than surface temperature, and this is true for

166   AMIP as well as for nature. Note that the noise turns out to be generally greater for larger domains

167   that include the extratropics as well as land. Note as well that this study deals with observed outgoing

168   fluxes, but does not specifically identify the origin of the changes.

169

170   **3. The data and their problems**

171   SST is measured (Kanamitsu *et al*., 2002), and is always fluctuating (viz. Fig. 2). To relate this

172   SST to the flux in the entire tropics, the SST anomaly was scaled by a factor of 0.78 (the area

173   fraction of the ocean to the tropics). High frequency fluctuations, however, make it difficult to

174   objectively identify the beginning and end of warming and cooling intervals (Trenberth *et al*., 2010).

175   This ambiguity is eliminated with a 3 point centered smoother (A two point lagged smoother works

176   too.). In addition, the net outgoing radiative flux from the earth has been monitored since 1985 by the

177   ERBE (Earth Radiation Budget Experiment) instrument (Barkstrom, 1984) (nonscanner edition 3)

178   aboard ERBS (Earth Radiation Budget Satellite) satellite, and since 2000 by the CERES (Clouds and

179   the Earth's Radiant Energy System) instrument (ES4 FM1 edition 2) aboard the Terra satellite

180   (Wielicki *et al*., 1998). The results for both LW radiation and SW radiation are shown in Fig. 3. The

181   sum is the net outgoing flux.

182   With ERBE data, there is the problem of satellite precession with a period of 72 days, although in

183   the deep tropics all clock hours are covered in 36 days. In Lindzen and Choi (2009) that used ERBE

184   data, we attempted to avoid this problem (which is primarily of concern for the short wave radiation)

185   by smoothing data over 7 months. It has been suggested (Murphy, 2010) that this is excessive

186   smoothing. In the present paper, we start by taking 36 day means rather than monthly means. The

187   CERES instrument is flown on a sun-synchronous satellite for which there is no problem with

188   precession. Thus for the CERES instrument we use the conventional months. However, here too, we

189   take a 3 point smoothing in the flux data to minimize the effect of noise. This is also why we use the

190   36-day averaged SST for 1985−1999 and monthly SST for 2000−2008 in Fig. 2.

191   The discontinuity between the two datasets requires comment. There is the long-term discrepancy

of the average which is believed to be due to the absolute calibration problem (up to 3 W m^{-2}) (Wong *et al.*, 2006). With CERES, we attempt to resolve the spectral darkening problem by multiplying SW flux by the scale factor (up to 1.011) from Matthews *et al*. (2005). However, this long-term stability should not matter for our analysis which only considers fluctuations over a few months for which the drift is insignificant. There is also the higher seasonal fluctuation in CERES SW radiation than in ERBE. The bias is up to 6.0 W m^{-2} as estimated by Young *et al*. (1998). This is attributed to different sampling patterns; i.e., ERBS observes all local times over a period of 72 days, while Terra observes the region only twice per day (around 10:30 AM and 10:30 PM). To avoid this problem, we reference the anomalies for radiative flux separately to the monthly means for the period of 1985 through 1989 for ERBE, and for the period of 2000 through 2004 for CERES. However, the issue of the reference period is also insignificant in this study since we use enough segments to effectively cancel out this seasonality.

The quality of ERBE and CERES data is best in the tropics for our feedback estimation. For latitudes 40° to 60°, 72 days are required instead of 36 days to reduce the precession effect (Wong *et al*., 2006). Both datasets have no or negligible shortwave radiation in winter hemispheric high latitudes. Also, the variations of solar irradiation that prevent distinguishing actual SW feedback always remain in the data partly including the extratropics. Moreover, our analysis involves relating changes in outgoing flux to changes in SST. This is appropriate to regions that are mostly ocean covered like the tropics or the southern hemisphere, but distinctly inappropriate to the northern extratropics. The effect of including extratropical data will, however, be discussed further in Sections 4-6.

Finally, there is the serious issue of distinguishing atmospheric phenomena involving changes in outgoing radiation that result from processes other than feedbacks (Pinatubo and non-feedback cloud variations for example) and which cause changes in SST, from those that are caused by changes in SST (namely the feedbacks we wish to evaluate) (Trenberth *et al*., 2010; Chung *et al*., 2010). Our

217 crude approach to this is to examine the effect of fluxes with time lags and leads relative to

218 temperature changes. The lags and leads examined are from one to five months. Our procedure will

219 be to choose lags that maximize R (the correlation). This is discussed in our section on methodology

220 (Section 4). To be sure, Fourier transform methods wherein one investigates phase leads and lags

221 might normally be cleaner, but, given the gaps in the radiation data as well as the incompatibilities

222 between ERBE and CERES, the present approach which focuses on individual warming and cooling

223 events seems more appropriate.

224   Turning to the models, AMIP is responsible for intercomparing atmospheric models used by the

225 IPCC (the Intergovernmental Panel on Climate Change); the AMIP models are forced by the same

226 observed SSTs shown in Fig. 2. We have obtained the calculated changes in both SW and LW

227 radiation from the AMIP models. These results are shown in Figs. 4 and 5 where the observed results

228 are also superimposed for comparison. We can already see that there are significant differences. In

229 addition, we will also consider results from CMIP (the Coupled Model Intercomparison Project),

230 where coupled ocean-atmosphere models were intercompared.

231

232 **4. Methodology**

233 *a. Feedback estimation method*

234   As already noted, the data need to be smoothed first to eliminate the ambiguity in choosing

235 segments. Then the procedure is simply to identify intervals of maximum change in ΔSST (red and

236 blue in Fig. 2), and for each such interval, to find the change in flux. The reasoning for this is that, by

237 definition, a temperature change is required to produce radiative feedback, and so the greatest signal

238 (and least noise) in the estimation of feedback should be associated with the largest temperature

239 changes. Thus, it is advisable, but not essential, to restrict oneself to changes greater than 0.1°C; in

240 fact, the impact of thresholds for ΔSST on the statistics of the results turns out, however, to be minor

241 (Lindzen and Choi, 2009).

242   Let us define t_1, t_2,…, t_m as selected time steps that correspond to the starting and the ending points

243   of intervals. Again, for stable estimation of ΔFlux/ΔSST, the time steps should be selected based on

244   the maximum and minimum of the 'smoothed' SST. In addition, if the maximum and minimum of

245   the smoothed SST appear at contiguous points or at points with no flux data (Fig. 3), we disregarded

246   them (black in Fig. 2). Specifically, we disregarded the beginning of the time series since the start

247   point of warming cannot be determined. Also, we disregarded the end of the time series since there

248   was missing data in radiative flux. Note that these disregarded periods include some intervals (e.g.,

249   the cooling SST in 1998) used in Lindzen and Choi (2009) where they selected neighboring end

250   points to avoid the missing flux data.

251   ΔFlux/ΔSST can be obtained by Flux(t_{i+1}) − Flux(t_i) divided by SST(t_{i+1}) − SST(t_i) where t_i is ith

252   selected time steps (i = 1, 2, …, m−1). As there are many intervals, the final ΔFlux/ΔSST is a

253   regression slope for the plots (ΔFlux, ΔSST) for a linear regression model. Here we use a zero y-

254   intercept model (y = ax) because the presence of the y-intercept is related to noise other than

255   feedbacks. Thus, a zero y-intercept model may be more appropriate for the purpose of our feedback

256   analysis though the choice of regression model turns out to also be minor in practice.

257   One must also distinguish ΔSST's that are forcing changes in ΔFlux, from responses to ΔFlux.

258   Otherwise, ΔFlux/ΔSST can have fluctuations (as found by Trenberth *et al*., 2010 and Dessler, 2010,

259   for example) that may not represent feedbacks that we wish to determine. The results from Trenberth

260   *et al*. (2010) and Dessler (2010) were, in fact, ambiguous as well because of the very low correlation

261   of their regression of ΔF on ΔSST. To avoid the causality problem, we use a lag-lead method (e.g.,

262   use of Flux(t+lag) and SST(t)) for ERBE 36-day and CERES monthly smoothed data). In general,

263   the use of leads for flux will emphasize forcing by the fluxes, and the use of lags will emphasize

264   responses by the fluxes to changes in SST.

265   The above procedures help to obtain a more accurate and objective climate feedback factor than

266   the use of original monthly data. As we will show below, this was tested by a Monte-Carlo test of a

267   simple feedback-forcing model.

268

269   *b. Simple model analysis*

270   Following Spencer and Braswell (2010), we assume an hypothetical climate system with uniform

271   temperature and heat capacity, for which SST and forcing are time-varying. Then the model equation

272   of the system is

273
$$C_p \left[\frac{d\Delta\text{SST}}{dt} \right] = Q(t) - F \cdot \Delta\text{SST}(t) \qquad (8)$$

274   where C_p is the bulk heat capacity of the system (14 yr W m^{-2} K^{-1} in this study, from Schwartz,

275   2007); ΔSST is SST deviation away from an equilibrium state of energy balance; F is the feedback

276   function that is the same as the definition in Eq. (2); Q is any forcing that changes SST (Forster and

277   Gregory, 2006; Spencer and Braswell, 2010). Q consists in three components: (i) Q_1=external

278   radiative forcing (e.g., from anthropogenic greenhouse gas emission.), (ii) Q_2=internal non-radiative

279   forcing (from heat transfer from the ocean, for example), and (iii) Q_3=internal radiative forcing (e.g.,

280   from water vapor or clouds.). Among the three forcings, the two external and internal 'radiative'

281   forcings, and $F \cdot \Delta$SST(t) constitute TOA net radiative flux anomaly; i.e., ΔFlux= $F \cdot \Delta$SST(t)-

282   [$Q_1(t)$+$Q_3(t)$].

283   The model system was basically forced by random internal non-radiative forcing changing SST (ie,

284   Q_2). The system was also forced by random internal radiative forcing (ie, Q_3). For this preliminary

285   test, normally distributed random numbers with zero mean were inserted into Q_1 and Q_2.; we

286   anticipate using forcing with realistic atmospheric or oceanic spectra in future tests. Here the

287   variance of internal non-radiative forcing is set to 5 and the variance of internal radiative forcing is

288   set to 0.7. Hence, the ratio of variances of the two forcings is 14% (hereafter the noise level). These

289   settings generally give simulated ΔSST and ΔFlux with similar variances to the observed, The

290   simulated variances are, however, subject to model representation as well. Finally the system was

291 additionally forced by transient external radiative forcing (0.4 W m^{-2} per decades due to increasing

292 CO$_2$) (Spencer and Braswell, 2010). Integration is done at monthly time steps[1]. We used Runge-

293 Kutta 4th order method for numerical solution of randomly forced system, Eq. (8) (Machiels and

294 Deville, 1998). Fig. 6 compares the simple regression method and our method for the feedback

295 function $F = 6$ W m^{-2} K^{-1} (it indicates negative feedback as it is larger than Planck response 3.3 W

296 m^{-2} K^{-1}). The maximum R occurs at small (zero or a month) lag and the corresponding ΔFlux/ΔSST

297 (5.7 W m^{-2} K^{-1}) is close to the assumed F (6 W m^{-2} K^{-1}), whereas the simple regression method

298 underestimates F (3.2 W m^{-2} K^{-1}).

299 The difference between the simple regression and our method is statistically significant by a

300 Monte-Carlo test (10,000 repetitions). Fig. 7 shows the probability density functions of the estimated

301 ΔFlux/ΔSST, and compares with the three true F values (1, 3.3, and 6 W m^{-2} K^{-1}) that were specified

302 for the model. We do not rule out the possibilities that both methods fail to estimate the actual

303 feedback (the tail of the density functions), but we see clearly that the simple regression always

304 underestimates negative feedbacks and exaggerates positive feedbacks. This is seen more clearly in

305 Table 1 which shows the central values of gain and feedback factors for both the simple regressions

306 and for the lag-lead approach (LC). The simple regression even finds fairly large positive feedbacks

307 when the actual feedback is negative. This bias is, at least, partially because the simple regression

308 includes time intervals that approach equilibration time, and at equilibrium, we would have a ΔSST

309 with no ΔFlux.

310 By contrast, our method shows moderately good performance for estimating the feedback

311 parameter especially for significant negative feedbacks (comparable to what we observe in the data).

312 The system with smaller F generates the sinusoidal shape of the slopes with respect to lags, so that it

313 turns out to have maximum R at larger lag. In this case, the estimated climate feedbacks are the

---

[1] It is also possible to integrate at daily time steps, and degrade the time series to the monthly
averages without significantly changing the results – suggesting that the coarser time resolution is

314 lagged response though estimates are less reliable than when maximum R occurs at near-zero lag

315 (Fig. 8). Therefore, for the system with smaller F our method is less efficient, and the true value is in

316 between the simple regression and our method. This is also the case for the system with the same F

317 with an increased noise level (Fig. 8). That is to say, the longer the lag needed to maximize R, the

318 more our method overestimates F. This may be because the lagged response is attributed to both

319 feedback and noise, and heavier noise at longer lag unduly raises the slope. Regardless of feedback

320 strength, with either no internal (cloud-induced) radiative change or the prescribed temperature

321 variation, ΔFlux/ΔSST at zero lag (with maximum R) is always identical to the assumed F. Thus

322 AMIP systematically shows maximum R at zero lag, while CMIP does not; thus, the use of AMIP

323 seems more appropriate in estimating model feedback than the use of CMIP.

324 An example of a comparison of simple regression with our lead-lag approach is taken from Choi *et*

325 *al*. (2011). Here we compared the use of the simple regression approach with our approach for the

326 complete CERES data set used by Dessler (2010). The results are shown in Fig. 9 where we

327 separately show the impact of using segments (as opposed to the continuous record as was done by

328 Dessler, 2010) and the use of lead-lag as opposed to simple regression. The former serves mainly to

329 greatly increase the correlation (r^2) from the negligible value obtained by Dessler (2010); the latter

330 leads to a significant negative feedback as opposed to the weak and insignificant positive feedback

331 claimed by Dessler (2010). We will discuss these results later in connection with our emphasis on

332 tropical data. Recall, that this example considers data from all latitudes covered by CERES.

333 However, it should be emphasized that even Dessler's treatment of the data leads to negative

334 feedback when lags are considered.

335

336 **5. Results**

337 *a. Climate sensitivity from observations and comparison to AMIP models*

---

adequate for our purposes.

338   Given the above, it is now possible to directly test the ability of models to adequately simulate the

339   sensitivity of climate (see Methodology, Section 4). Fig. 10 shows the impact of smoothing and leads

340   and lags on the determination of the slope as well as on the correlation, R, of the linear regression.

341   For LW radiation, the situation is fairly simple. Smoothing increases R somewhat, and for 3 point

342   symmetric smoothing, R maximizes for slight lag or zero – consistent with the fact that feedbacks are

343   expected to result from fast processes. Maximum slope is found for a lag of 1 'month', though it

344   should be remembered that the relevant feedback processes may operate on a time scale shorter than

345   we resolve. The situation for SW radiation is, not surprisingly, more complex since phenomena like

346   the Pinatubo eruption and non-feedback cloud fluctuations lead to changes in SW reflection and

347   associated fluctuations in surface temperature.

348   We see two extrema associated with changing lead/lag. There is a maximum negative slope

349   associated with a brief lead, and a relatively large positive slope associated with a 3–4 month lag.

350   The lags in SW that maximize R are rather long compared to what we get with the simple model.

351   This is because the simple model is of total radiation with Planck response. Consistently, the

352   summation of LW and SW radiations presents a shorter lag. It seems reasonable to suppose that the

353   effect of anomalous forcing extends into the results at small lags because it takes time for the ocean

354   surface to respond, and is only overcome for larger lags where the change in flux associated with

355   feedback dominates. Indeed, excluding the case of the Pinatubo volcano for larger lags does little to

356   change the results (less than 0.3 W m^{-2} K^{-1}). Under such circumstances, we expect the maximum

357   slope for SW radiation in Fig. 10 to be an underestimate of the actual feedback (for reasons we

358   discussed in Section 4b). We also consider the standard error of the slope to show data uncertainty.

359   The results for the lags associated with maximum R are shown in Table 2. We take LW and SW

360   radiation for lag = 1 and lag = 3, respectively, and measure the slope ΔFlux/ΔSST for the sum of

361   these fluxes. The standard error of the slope in total radiation for the appropriate lags comes from the

362   regression for scatter plots of (ΔSST, Δ(OLR+SWR)). With the slope and its standard error, the

15

363   feedback factors for LW, SW, and total radiation (f_{SW}, f_{LW}, and f_{Total}) are obtained via Eqs. (6) and (7).

364   Finally, with f_{Total}, the equilibrium climate sensitivity for a doubling of CO_2 is obtained via Eq. (3).

365   Here the statistical confidence intervals of the sensitivity estimate at 90%, 95%, and 99% levels are

366   also calculated by the standard error of the feedback factor f_{Total}. This interval should prevent any

367   problems arising from limited sampling. As a result, the climate sensitivity for a doubling of CO_2 is

368   estimated to be 0.7K (with the confidence interval 0.5K−1.3K at 99% levels). This observational

369   result shows that model sensitivities indicated by the IPCC AR4 are likely greater than the

370   possibilities estimated from the observations.

371   We next wish to see whether the outgoing fluxes from the AMIP models are consistent with the

372   sensitivities in IPCC AR4. To the AMIP results, for which there was less ambiguity as to whether

373   fluxes constituted a response (noise still exists due to autonomous cloud fluctuations), the same

374   approach as that for the observations was applied. Maximum R occurs at zero lag in both LW and

375   SW radiation, so we simply chose the AMIP fluxes without lag. The results are shown in Table 3. In

376   contrast to the observed fluxes, the implied feedbacks in the models are all positive, and in one case,

377   marginally unstable. Given the uncertainties, however, one should not take that too seriously.

378   Table 4 compares the climate sensitivities in degrees K for a doubling of CO_2 implied by feedback

379   factors f in Table 3 with those in IPCC AR4. To indicate statistical significance of our results

380   obtained from limited sampling, we also calculated the confidence intervals of the climate sensitivity

381   using the standard errors of f in Table 3. All the sensitivities in IPCC AR4 are within the 90%

382   confidence intervals of our sensitivity estimates. The agreement does not seem notable, but this is

383   because, for positive feedbacks, sensitivity is strongly affected by small changes in f that are

384   associated standard errors in Table 3. Consequently, the confidence intervals include "infinity". This

385   is seen in Fig. 11 in the pink region. It has, in fact, been suggested by Roe and Baker (2007), that this

386   sensitivity of the climate sensitivity to uncertainty in the feedback factor is why there has been no

387   change in the range of climate sensitivities indicated by GCMs since the 1979 Charney Report

388 (1979). By contrast, in the green region, which corresponds to the observed feedback factors,

389 sensitivity is much better constrained.

390   While the present analysis is a direct test of feedback factors, it does not provide much insight into

391 detailed mechanism. Nevertheless, separating the contributions to f from long wave and short wave

392 fluxes provides some interesting insights. The results are shown in Tables 2 and 3. It should be noted

393 that the consideration of the zero-feedback response, and the tropical feedback factor to be half of the

394 global feedback factor is actually necessary for our measurements from the Tropics; however, these

395 were not considered in Lindzen and Choi (2009). Accordingly, with respect to separating longwave

396 and shortwave feedbacks, the interpretation by Lindzen and Choi (2009) needs to be corrected. These

397 tables show recalculated feedback factors in the presence of the zero-feedback Planck response. The

398 negative feedback from observations is from both longwave and shortwave radiation, while the

399 positive feedback from models is usually but not always from longwave feedback.

400   As concerns the infrared, there is, indeed, independent evidence for a positive water vapor

401 feedback (Soden *et al.*, 2005), but, if this is true, this feedback is presumably cancelled by a negative

402 infrared feedback such as that proposed by LCH01 on the iris effect. In the models, on the contrary,

403 the long wave feedback appears to be positive (except for two models), but it is not as great as

404 expected for the water vapor feedback (Colman, 2003; Soden *et al.*, 2005). This is possibly because

405 the so-called lapse rate feedback as well as negative longwave cloud feedback acting to cancel some

406 of the TOA OLR feedback in current models. Table 3 implies that TOA longwave and shortwave

407 contributions are coupled in models (the correlation coefficient between f_{LW} and f_{SW} from models is

408 about −0.5.). This coupling most likely is associated with the primary clouds in models — optically

409 thick high-top clouds (Webb *et al.*, 2006). In most climate models, the feedbacks from these clouds

410 are simulated to be negative in longwave and strongly positive in shortwave, and dominate the entire

411 model cloud feedback (Webb *et al.*, 2006). Therefore, the cloud feedbacks may also serve to

412 contribute to the negative OLR feedback and the positive SWR feedback. New spaceborne data from

17

413   the CALIPSO lidar (CALIOP; Winker *et al*., 2007) and the CloudSat radar (CPR; Im *et al*., 2005)

414   should provide a breakdown of cloud behavior with altitude which may give some insight into what

415   actually is contributing to the radiation.

416

417   *b. Comparison to CMIP models and their limitations*

418   It has been argued that CMIP models are more appropriate for the present purpose since the

419   uncoupled AMIP models are prescribed with incomplete forcings of SST (Trenberth *et al*., 2010).

420   However, it is precisely for this reason that AMIP models are preferred for feedback estimates. Note

421   that we are considering atmospheric feedbacks to SST fluctuations. As already seen, in analyzing

422   observed behavior, the presence of SST variations that are primarily caused by atmospheric changes

423   (from volcanoes, non-feedback cloud variations, etc.) leads to difficulty in distinguishing SST

424   variations that are primarily forcing atmospheric changes (i.e., feedbacks). This situation is much

425   simpler with AMIP results since we can be sure that SST variations (which are forced to be the same

426   as observed SST) cannot respond to atmospheric changes. The fact that CMIP SST variations are

427   significantly different from observed SST variations further makes it unlikely that the model

428   atmospheric processes are implicitly forcing the SST's used for AMIP. Note that important ocean

429   phenomena such as El Niño-Southern Oscillation and Pacific Decadal Oscillation are generally

430   misrepresented by CMIP models. As noted, AMIP results are still subject to noise since outgoing

431   radiation includes changes associated with non-feedback cloud variations.

432   In applying our methodology to CMIP, we see that coupled models differ in the behavior of SST,

433   and the intervals of SST must be selected differently for different models. Some models have much

434   smaller variability of SST than nature and only a few intervals of SST could be selected. As we see

435   in Fig. 12, the CMIP results (black dots) display behavior somewhat similar to ERBE and CERES

436   results (red open circles) with respect to lags. However, when identifying each number, we found

437   that the results are quantitatively ambiguous. The slope $\Delta OLR/\Delta SST$ for lag $= 1$ is between 0.6 and

438   5.8 though it remains robust that LW feedbacks in most models are higher than nature. Not

439   surprisingly, the inconsistent LW feedback was also shown in previous studies (Tsushima *et al.*,

440   2005; Forster and Gregory, 2006; Forster and Taylor, 2006). The slope $\Delta SWR/\Delta SST$ for lag = 3 is

441   between −3.4 and 3.9 so that one cannot meaningfully determine the feedback in the models. These

442   values, moreover, do not correspond well to the independently known model climate sensitivities in

443   IPCC AR4. Based on our simple model (viz Section 4b of Methodology), this ambiguity results

444   mainly from non-feedback internal radiative (cloud-induced) change that changes SST. Also, such

445   cloud-induced radiative change can generate the anomalous sinusoidal shape of the slopes

446    $\Delta SWR/\Delta SST$ with respect to lags as shown in Fig. 12. Therefore, previous studies that use the slopes

447    $\Delta SWR/\Delta SST$ at zero lag (Tsushima *et al.*, 2005; Forster and Gregory, 2006; Trenberth *et al*., 2010)

448   may misinterpret SW feedback. This confirms that for more accurate estimation of 'model'

449   feedbacks, AMIP models are more appropriate than CMIP models. Furthermore, nature is better than

450   CMIP for SST simply because nature properly displays the real magnitude of SST forcing and the

451   associated atmospheric changes.

452

453   **6. Conclusions and discussions**

454   We have corrected the approach of Lindzen and Choi (2009), based on all the criticisms made of

455   the earlier work (Trenberth *et al*., 2010; Chung et al., 2010; Murphy, 2010). First of all, to improve

456   the statistical significance of the results, we supplemented ERBE data with CERES data, filtered out

457   data noise with 3-month smoothing, objectively chose the intervals based on the smoothed data, and

458   provided confidence intervals for all sensitivity estimates. These constraints helped us to more

459   accurately obtain climate feedback factors than with the original use of monthly data. Next, our new

460   formulas for climate feedback and sensitivity reflect sharing of tropical feedback with the globe, so

461   that the tropical region is now properly identified as an open system. Last, the feedback factors

462   inferred from the atmospheric models are more consistent with IPCC-defined climate sensitivity than

463   those from the coupled models. This is because, in the presence of cloud-induced radiative changes

464   altering SST, the climate feedback estimates by the present approach tends to be inaccurate. With all

465   corrections, the conclusion still appears to be that all current models seem to exaggerate climate

466   sensitivity (some greatly). Moreover, we have shown why studies using simple regressions of ΔFlux

467   on ΔSST serve poorly to determine feedbacks.

468   To respond to the criticism of our emphasis on the tropical domain (Trenberth *et al.*, 2010;

469   Murphy, 2010), we analyzed the complete record of CERES for the globe (Dessler, 2010) (Note that

470   ERBE data is not available for the high latitudes since the field-of-view is between 60°S and 60°N).

471   As seen in the previous section, the use of the global CERES record leads to a result that is basically

472   similar to that from the tropical data in this study . The global CERES record, however, contains

473   more noise than the tropical record.

474   This result lends support to the argument that the water vapor feedback is primarily restricted to

475   the tropics, and there are reasons to suppose that this is also the case for cloud feedbacks. Although,

476   in principle, climate feedbacks may arise from any latitude, there are substantive reasons for

477   supposing that they are, indeed, concentrated mostly in the tropics. The most prominent model

478   feedback is that due to water vapor, where it is commonly noted that models behave roughly as

479   though relative humidity were fixed. Pierrehumbert (2009) examined outgoing radiation as a function

480   of surface temperature theoretically for atmospheres with constant relative humidity. His results are

481   shown in Fig. 13.

482   Specific humidity is low in the extratropics, while it is high in the tropics. We see that for

483   extratropical conditions, outgoing radiation closely approximates the Planck black body radiation

484   (leading to small feedback). However, for tropical conditions, increases in outgoing radiation are

485   suppressed, implying substantial positive feedback. There are also reasons to suppose that cloud

486   feedbacks are largely confined to the tropics. In the extratropics, clouds are mostly stratiform clouds

487   that are associated with ascending air while descending regions are cloud-free. Ascent and descent

488 are largely determined by the large scale wave motions that dominate the meteorology of the

489 extratropics, and for these waves, we expect approximately 50% cloud cover regardless of

490 temperature (though details may depend on temperature). On the other hand, in the tropics, upper

491 level clouds, at least, are mostly determined by detrainment from cumulonimbus towers, and cloud

492 coverage is observed to depend significantly on temperature (Rondanelli and Lindzen, 2008).

493 As noted by LCH01, with feedbacks restricted to the tropics, their contribution to global

494 sensitivity results from sharing the feedback fluxes with the extratropics. This led to inclusion of the

495 sharing factor c in Eq. (6). The choice of a larger factor c leads to a smaller contribution of tropical

496 feedback to global sensitivity, but the effect on the climate sensitivity estimated from the observation

497 is minor. For example, with $c = 3$, climate sensitivity from the observation and the models is 0.8 K

498 and a higher value (between 1.3 K and 6.4 K), respectively. With $c = 1.5$, global equilibrium

499 sensitivity from the observation and the models is 0.6 K and any value higher than 1.6 K,

500 respectively. Note that, as in LCH01, we are not discounting the possibility of feedbacks in the

501 extratropics, but rather we are focusing on the tropical contribution to global feedbacks. Note that,

502 when the dynamical heat transports toward the extratropics are taken into account, the overestimation

503 of tropical feedback by GCMs may lead to even greater overestimation of climate sensitivity (Bates,

504 2011). This emphasizes the importance of the tropical domain itself.

505 Our analysis of the data only demands relative instrumental stability over short periods, and is

506 largely independent of long term drift. Concerning the different sampling from the ERBE and

507 CERES instruments, Murphy et al. (2009) repeated the Forster and Gregory (2006) analysis for the

508 CERES and found very different values than those from the ERBE. However, in this study, the

509 addition of CERES data to the ERBE data does little to change the results for ΔFlux/ΔSST – except

510 that its value is raised a little (as is also true when only CERES data is used.). This may be because

511 these previous simple regression approaches include the distortion of feedback processes by

512 equilibration. In distinguishing a precise feedback from the data, the simple regression method is

513   dependent on the data period, while our method is not. The simple regression result in Fig. 7 is worse

514   if the model integration time is longer (probably due to the greater impact of increasing radiative

515   forcing).

516   Our study also suggests that, in current coupled atmosphere-ocean models, the atmosphere and

517   ocean are too weakly coupled since thermal coupling is inversely proportional to sensitivity (Lindzen

518   and Giannitsis, 1998). It has been noted by Newman et al. (2009) that coupling is crucial to the

519   simulation of phenomena like El Niño. Thus, corrections of the sensitivity of current climate models

520   might well improve the behavior of coupled models, and should be encouraged. It should be noted

521   that there have been independent tests that also suggest sensitivities less than predicted by current

522   models. These tests are based on the response to sequences of volcanic eruptions (Lindzen and

523   Giannitsis, 1998), on the vertical structure of observed versus modeled temperature increase

524   (Lindzen, 2007; Douglass, 2007), on ocean heating (Schwartz, 2007; Schwartz, 2008), and on

525   satellite observations (Spencer and Braswell, 2010). Most claims of greater sensitivity are based on

526   the models that we have just shown can be highly misleading on this matter. There have also been

527   attempts to infer sensitivity from paleoclimate data (Hansen *et al*., 1993), but these are not really

528   tests since the forcing is essentially unknown given major uncertainties in clouds,dust loading and

529   other factors. Finally, we have shown that the attempts to obtain feedbacks from simple regressions

530   of satellite measured outgoing radiation on SST are inappropriate.

531   One final point needs to be made. Low sensitivity of global mean temperature anomaly to global

532   scale forcing does not imply that major climate change cannot occur. The earth has, of course,

533   experienced major cool periods such as those associated with ice ages and warm periods such as the

534   Eocene (Crowley and North, 1991). As noted, however, in Lindzen (1993), these episodes were

535   primarily associated with changes in the equator-to-pole temperature difference and spatially

536   heterogeneous forcing. Changes in global mean temperature were simply the residue of such changes

537   and not the cause.

538

546

547   **References**

548   Bates, R. (2011), Climate stability and Sensitivity in some simple conceptual models. *Climate Dyn.*,

549   in press.

550   Barkstrom, B. R. (1984) The Earth Radiation Budget Experiment (ERBE). *Bull. Amer. Met. Soc.*, **65**,

551   1170–1185.

552   Charney J. G. *et al.*, 1979: *Carbon dioxide and climate: a scientific assessment*, National Research

553   Council, Ad Hoc Study Group on Carbon Dioxide and Climate. National Academy Press,

554   Washington, DC, 22 pp.

555   Choi, Y.-S., H. Cho, C.-H. Ho, R. S. Lindzen, and S.-K. Park, 2011: Comments on "a determination

556   of the cloud feedback from climate variations over the past decade". *science*, revised.

557   Chung, E.-S., B. J. Soden, and B. J. Sohn, 2010: Revisiting the determination of climate sensitivity

558   from relationships between surface temperature and radiative fluxes. *Geophys. Res. Lett.*, **37**,

559   L10703.

560   Colman, R., 2003: A comparison of climate feedbacks in general circulation models. *Climate Dyn.*,

561   **20,** 865–873.

562   Crowley, T. J., and G. R. North, 1991: *Paleoclimatology.* Oxford Univ Press, NY, 339 pp.

563   Dessler, A. E., 2010: A determination of the cloud feedback from climate variations over the past

564   decade. *Science*, **330**, 1523-1527.

565   Douglass, D. H., J. R. Christy, B. D. Pearson, and S. F. Singer, 2007: A comparison of tropical

566   temperature trends with model predictions. *Int. J. Climatol* 28, 1693–1701.

567   Forster, P. M., and J. M. Gregory, 2006: The climate sensitivity and its components diagnosed from

568   Earth Radiation Budget data. *J. Climate.*, **19**, 39−52.

569   ____, and K. E. Taylor, 2006: Climate forcing and climate sensitivities diagnosed from coupled

570   climate model integrations. *J. Climate*, **19**, 6181−6194.

571   Hansen, J. *et al.*, 1993: How sensitive is the world's climate? *Natl. Geogr. Res. Explor.* 9, 142–158.

572   Hartmann, D. L., 1994: Global physical climatology. Academic Press, 411 pp.

573   Im, E, S. L. Durden, and C. Wu, 2005: Cloud profiling radar for the Cloudsat mission. *IEEE Trans.*

574   *Aerosp. Electron. Syst.*, **20**, 15–18.

575   Intergovernmental Panel on Climate Change, 2007: Climate Change 2007: The Physical Science

576   Basis. Contribution of Working Group I to the Fourth Assessment Report of the

577   Intergovernmental Panel on Climate Change. Cambridge Univ. Press, Cambridge, U. K.

578   Kanamitsu, M, *et al.*, 2002: NCEP/DOE AMIP-II Reanalysis (R-2). *Bull. Amer. Met. Soc.*, **83**, 1631–

579   1643.

580   Lindzen, R. S., A. Y. Hou, and B. F. Farrell, 1982: The role of convective model choice in

581   calculating the climate impact of doubling CO_2. *J. Atmos. Sci.*, **39**, 1189-1205.

582   ____, 1999: The Greenhouse Effect and its problems. Chapter 8 in *Climate Policy After Kyoto* (T.R.

583   Gerholm, editor), Multi-Science Publishing Co., Brentwood, UK, 170 pp.

584   ____, 1993: Climate dynamics and global change. *Ann. Rev. Fl. Mech.* 26, 353–378.

585   ____, C. Giannitsis, 1998: On the climatic implications of volcanic cooling. *J. Geophys. Res.*, **103**,

586   5929–5941.

587   ____, M.-D. Chou, and A. Y. Hou, 2001: Does the Earth have an adaptive infrared iris? *Bull. Amer.*

588   *Met. Soc.*, **82**, 417–432.

589   ____, 2007: Taking greenhouse warming seriously. *Energy & Environment*, **18**, 937–950.

590   ____, and Y.-S. Choi, 2009: On the determination of climate feedbacks from ERBE data. *Geophys.*

591   *Res. Lett.*, **36**, L16705.

592   Machiels and Deville, Numerical simulation of randomly forced turbulent flows. *J. Comput, Physics*,

593   145, 246–279.

594   Matthews, G. *et al.*, 2005: "Compensation for spectral darkening of short wave optics occurring on

595   the Clouds and the Earth's Radiant Energy System," in *Earth Observing Systems* X, edited by

596   James J. Butler, Proceedings of SPIE Vol. 5882 (SPIE, Bellingham, WA) Article 588212.

597   Murphy, D. M. *et al*., 2009: An observationally based energy balance for the Earth since 1950. *J.*

598   *Geophys. Res.* **114**, D17107.

599   ____, 2010: Constraining climate sensitivity with linear fits to outgoing radiation. *Geophys. Res.*

600   *Lett.*, **37**, L09704.

601   Newman, M., P. D. Sardeshmukh, and C. Penland, 2009: How important is air-sea coupling in ENSO

602   and MJO Evolution? *J. Climate*, **22**, 2958–2977.

603   Pierrehumbert, R. T., 2009: Principles of planetary climate. Cambridge University Press, 688 pp.

604   Roe, G. H., and M. B. Baker, 2007: Why is climate sensitivity so unpredictable? *Science*, **318**, 629-

605   632.

606   Rondanelli, R., and R. S. Lindzen, 2008: Observed variations in convective precipitation fraction and

607   stratiform area with sea surface temperature. *J. Geophys. Res.*, **113**, D16119.

608   Schwartz, S. E., 2007: Heat capacity, time constant, and sensitivity of Earth's climate system. *J.*

609   *Geophy. Res.*, **112**, D24S05.

610   ____, 2008: Reply to comments by G. Foster et al., R. Knutti et al., and N. Scafetta, on "Heat

611   capacity, time constant, and sensitivity of Earth's climate system*". J. Geophys. Res.*, **113**,

612   D15195.

613   Soden, B. J., D. L. Jackson, V. Ramaswamy, M. D. Schwarzkopf, and X. Huang, 2005: The radiative

614   signature of upper tropospheric moistening. *Science*, **310**, 841–844.

615   Spencer R. W., and W. D. Braswell, 2010: On the diagnosis of radiative feedback in the presence of

616   unknown radiative forcing. *J. Geophys. Res.*, **115**, D16109.

617   Trenberth, K. E., J. T. Fasullo, C. O'Dell, and T. Wong, 2010: Relationships between tropical sea

618   surface temperature and top-of-atmosphere radiation. *Geophys. Res. Lett.*, **37**, L03702.

619   Tsushima, Y., A. Abe-Ouchi, and S. Manabe, 2005: Radiative damping of annual variation in global

620   mean surface temperature: comparison between observed and simulated feedback. *Clim. Dyn*.

621   **24**(6): 591–597.

622   Wielicki, B. A. *et al*., 1998: Clouds and the Earth's Radiant Energy System (CERES): Algorithm

623   overview. *IEEE Trans. Geosci. Remote. Sens.* **36**, 1127–1141.

624   Wong, T. *et al*., 2006: Reexamination of the observed decadal variability of the earth radiation

625   budget using altitude-corrected ERBE/ERBS nonscanner WFOV Data. *J. Climate*, **19**, 4028–

626   4040.

627   Webb, M. J. *et al*., 2006: On the contribution of local feedback mechanisms to the range of climate

628   sensitivity in two GCM ensembles. *Clim. Dyn.* **27**, 17–38.

629   Winker, D. M., W. H. Hunt, and M. J. McGill, 2007: Initial performance assessment of CALIOP.

630   *Geophys. Res. Lett.*, **34**, L19803.

631   Young, D. F. *et al*., 1998: Temporal Interpolation Methods for the Clouds and Earth's Radiant

632   Energy System (CERES) Experiment. *J. Appl. Meteorol.*, **37**, 572–590.

633

Table Legends

Table 1. Summary of simple model simulation results shown in Fig. 7. The gain is $1/G_0$ divided by the averaged F. Note that the averaged F is larger than the value of the most frequent occurrence for the simple regression method.

Table 2. Mean±standard error of the variables for the likely lag for the observations. The units for the slope are W m^{-2} K^{-1}. Also shown are the estimated mean and range of equilibrium climate sensitivity (in K) for a doubling of CO_2 for 90%, 95%, and 99% confidence levels. The numbers are basically calculated to the second decimal place, and then presented as the first decimal place in this table. The mean f_{Total} is actually -0.54.

Table 3. Regression statistics between ΔFlux and ΔSST and the estimated feedback factors (f) for LW, SW, and total radiation in AMIP models; the slope is ΔFlux/ΔSST, N is the number of the points or intervals, R is the correlation coefficient, and SE is the standard error of ΔFlux/ΔSST.

Table 4. Comparison of model equilibrium climate sensitivities (in K) for a doubling of CO_2 defined from IPCC AR4 and estimated from feedback factors in this study. The obvious difference between two columns labeled 'sensitivity' is discussed in more detail in the last paragraph of section 3.1. The estimated climate sensitivities for models as well as their confidence intervals are given for 90%, 95%, and 99% confidence levels.

652 Table 1

True values		LC		Simple regression	
Gain	f	Gain	f	Gain	f
0.55	−0.80	0.52	−0.92	0.66	−0.51
1.00	0.00	0.83	−0.21	1.42	0.29
3.30	0.68	1.53	0.34	23.57	0.94

653

654 Table 2

	Variables		Comments
a	Slope, LW	5.3±1.3	Lag = 1
b	Slope, SW	1.9±2.6	Lag = 3
c	Slope, Total	6.9±1.8	= a+b for the same SST interval
d	f_{LW}	−0.3±0.2	Calculated from a
e	f_{SW}	−0.3±0.4	Calculated from b
f	f_{Total}	−0.5±0.3	Calculated from c
g	Sensitivity, mean	0.7	Calculated from f
h	Sensitivity, 90%	0.6–1.0	Calculated from f
i	Sensitivity, 95%	0.5–1.1	Calculated from f
j	Sensitivity, 99%	0.5–1.3	Calculated from f

655

656 Table 3

	N	LW				SW				LW+SW			
		Slope	R	SE	f_{LW}	Slope	R	SE	f_{SW}	Slope	R	SE	f
CCSM3	17	1.2	0.4	2.0	0.3	−3.7	−0.9	1.0	0.6	−2.5	−0.5	2.2	0.9
ECHAM5/MPI-OM	16	1.1	0.4	1.6	0.3	−0.1	0.0	1.9	0.0	1.0	0.3	2.1	0.3
FGOALS-g1.0	16	0.4	0.2	1.2	0.4	−2.8	−0.8	1.0	0.4	−2.4	−0.6	1.4	0.9
GFDL-CM2.1	16	2.1	0.8	0.9	0.2	−2.1	−0.4	2.4	0.3	0.0	0.0	2.0	0.5
GISS-ER	21	3.2	0.8	1.1	0.0	−3.7	−0.6	1.8	0.6	−0.5	−0.1	1.3	0.6
INM-CM3.0	23	2.7	0.6	1.4	0.1	−3.4	−0.7	1.3	0.5	−0.7	−0.1	1.8	0.6
IPSL-CM4	21	−0.4	−0.1	1.1	0.6	−2.3	−0.5	1.6	0.3	−2.7	−0.5	1.7	0.9
MRI-CGCM2.3.2	21	−0.8	−0.3	1.3	0.6	−3.8	−0.6	2.5	0.6	−4.7	−0.7	2.5	1.2
MIROC3.2(hires)	21	2.4	0.6	1.4	0.1	−2.4	−0.7	1.4	0.4	0.0	0.0	1.3	0.5
MIROC3.2(medres)	21	3.4	0.8	1.0	0.0	−3.6	−0.7	2.0	0.5	−0.3	−0.1	1.6	0.5
UKMO-HadGEM1	17	4.4	0.8	2.2	−0.2	−3.6	−0.7	1.5	0.5	0.8	0.2	2.1	0.4

657

658 Table 4

Models	IPCC AR4	Estimate in this study		
	Sensitivity	Sensitivity	Confidence interval of sensitivity	
			90%	95%	99%
CCSM3	2.7	8.1	1.6 – Infinity	1.4 – Infinity	1.1 – Infinity
ECHAM5/MPI-OM	3.4	1.7	0.9 – 8.0	0.9 – 28.2	0.8 – Infinity
FGOALS-g1.0	2.3	7.9	2.2 – Infinity	2.0 – Infinity	1.6 – Infinity
GFDL-CM2.1	3.4	2.2	1.1 – 351.4	1.0 – Infinity	0.8 – Infinity
GISS-ER	2.7	2.5	1.5 – 8.7	1.4 – 16.4	1.2 – Infinity
INM-CM3.0	2.1	2.7	1.3 – Infinity	1.2 – Infinity	1.0 – Infinity
IPSL-CM4	4.4	10.4	2.1 – Infinity	1.8 – Infinity	1.4 – Infinity
MRI-CGCM2.3.2	3.2	Infinity	2.5 – Infinity	2.0 – Infinity	1.4 – Infinity
MIROC3.2(hires)	4.3	2.2	1.3 – 6.4	1.2 – 10.0	1.1 – Infinity
MIROC3.2(medres)	4	2.4	1.3 – 14.7	1.2 – Infinity	1.0 – Infinity
UKMO-HadGEM1	4.4	1.7	1.0 – 8.8	0.9 – 38.9	0.8 – Infinity

659

Figure Legends

Fig. 1. A schematic for the behavior of the climate system in the absence of feedbacks (a), in the

presence of feedbacks (b).

Fig. 2. Tropical mean (20°S to 20°N latitude) 36-day averaged and monthly sea surface temperature

anomalies with the centered 3-point smoothing; the anomalies are referenced to the monthly means

for the period of 1985 through 1989. Red and blue colors indicate the major temperature fluctuations

exceeding 0.1°C used in this study. The cooling after 1998 El Niño is not included because of no flux

data is available for this period (viz. Fig. 3).

Fig. 3. The same as Fig. 2 but for outgoing longwave (red) and reflected shortwave (blue) radiation

from ERBE and CERES satellite instruments. 36-day averages are used to compensate for the ERBE

precession. The anomalies are referenced to the monthly means for the period of 1985 through 1989

for ERBE, and 2000 through 2004 for CERES. Missing periods are the same as reported in ref. 17.

Fig. 4 Comparison of outgoing longwave radiation from AMIP models (black) and the observations

(red) shown in Fig. 3.

Fig. 5 Comparison of reflected shortwave radiation from AMIP models (black) and the observations

(blue) shown in Fig. 3.

Fig. 6. Comparison between simple regression method and the method used in this study, based on

simple model results.

Fig. 7. Probability density function of simple model simulation results (10,000 repeats) for the

feedback parameter $F = 1$, 3.3, and 6 $Wm^{-2}K^{-1}$ (blue dotted line). The black line is from the simple

regression, and the red line is from the methodology in this study. Note that, in the case of 'true'

positive feedback, the LC method shows an insignificant indication of a negative feedback. The

means of the lags with maximum R selected in our method are also noted.

Fig. 8. The relationship between the estimated feedback parameter F, the lags with maximum R, and

the noise level (in %).

685   **Fig. 9**. (a) Scatter plots and regression lines of radiative flux variation by clouds (ΔR_{cloud}) versus ΔT

686   from CERES and ECMWF interim data used in Dessler (2010). ΔR_{cloud} and ΔT values are calculated

687   by taking (black) original monthly anomaly data, and (red) the method in this study. (b) The slopes

688   and their one-σ uncertainties of lagged linear regressions of ΔR_{cloud} versus ΔT_s; the numbers indicate

689   lagged linear correlation coefficients [Taken from Choi *et al*. (2011)].

690   **Fig. 10**. The impact of smoothing and leads and lags on the determination of the slope (top) as well

691   as on the correlation coefficient, R, of the linear regression (bottom).

692   **Fig. 11**. Sensitivity vs. feedback factor.

693   **Fig. 12.** Same as Fig. 4, but for the 10 CMIP models (black dots); GISS model was excluded because

694   only few intervals of SST are obtained. The values for the 3-month smoothing in Fig. 4 are

695   superimposed by red dots.

696   **Fig. 13**. OLR vs. surface temperature for water vapor in air, with relative humidity held fixed. The

697   surface air pressure is 1bar. The temperature profile is the water/air moist adiabat. Calculations were

698   carried out with the Community Climate Model radiation code (Pierrehumbert, 2009).

699

700

(a)

ΔQ ΔQ

G_0 ΔT_0

(b)

ΔQ

G_0 ΔT

$\Delta T = G_0(\Delta Q + F\Delta T)$

F

$F\Delta T$
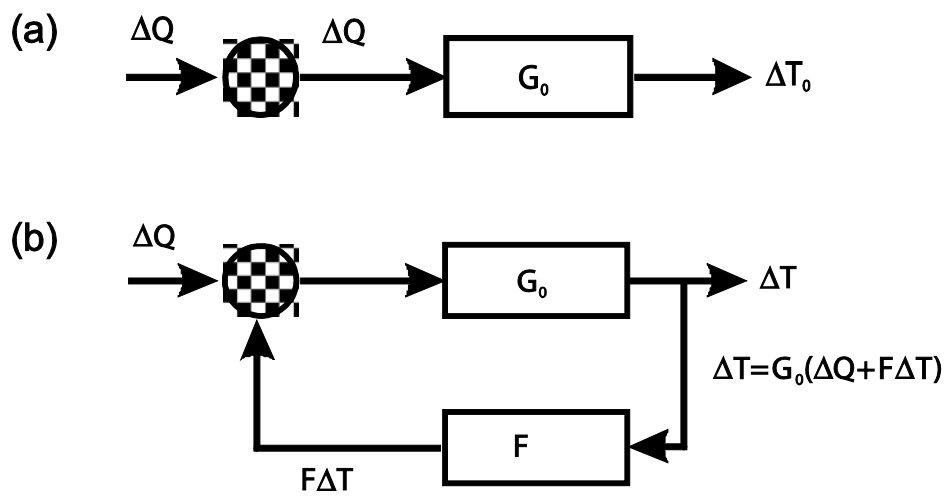
701

702   Figure 1

703
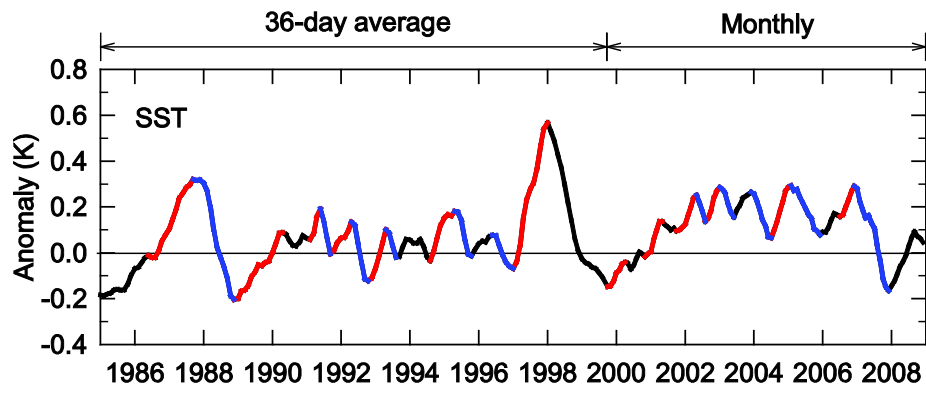
704

705   Figure 2
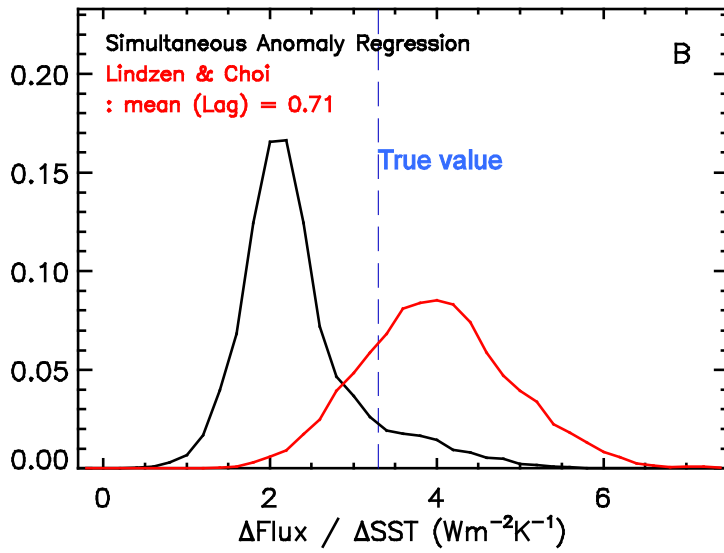
706
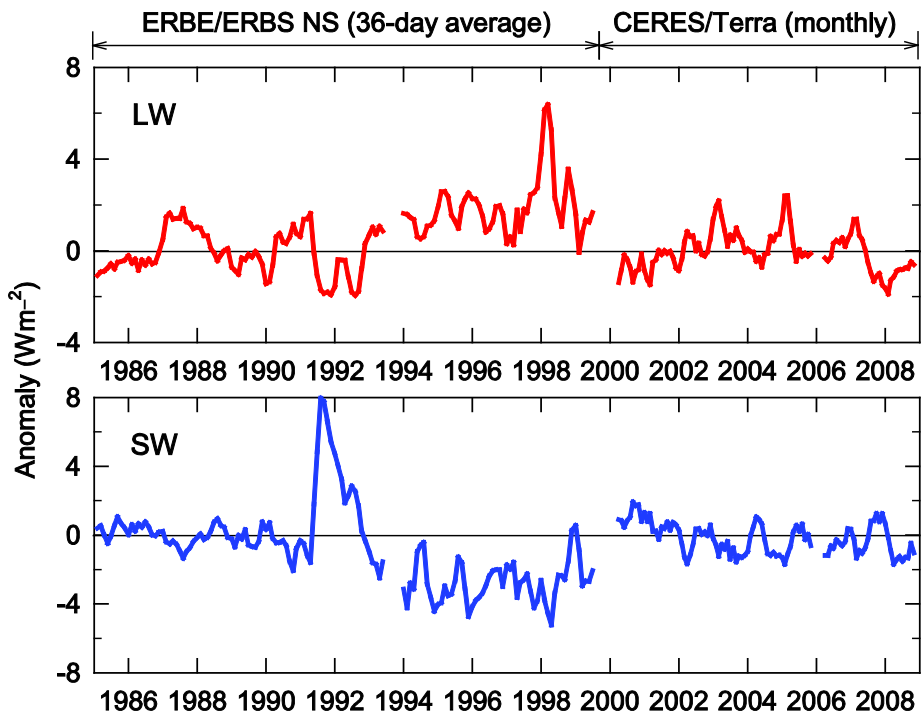
707

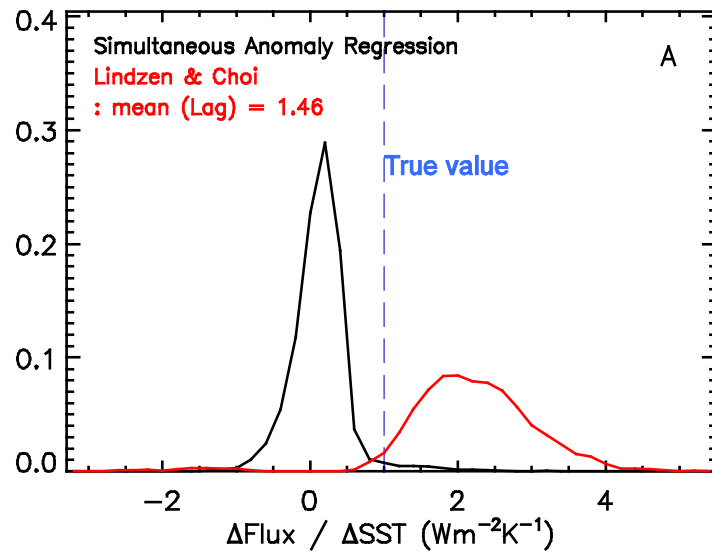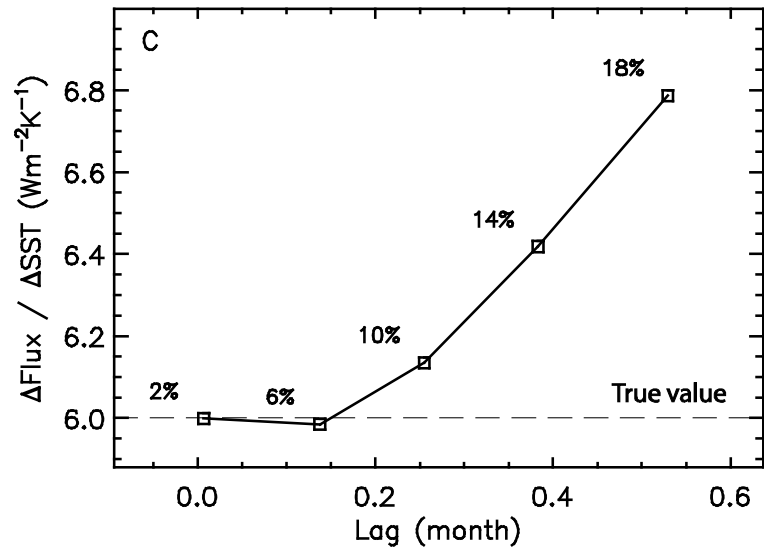708   Figure 3

709
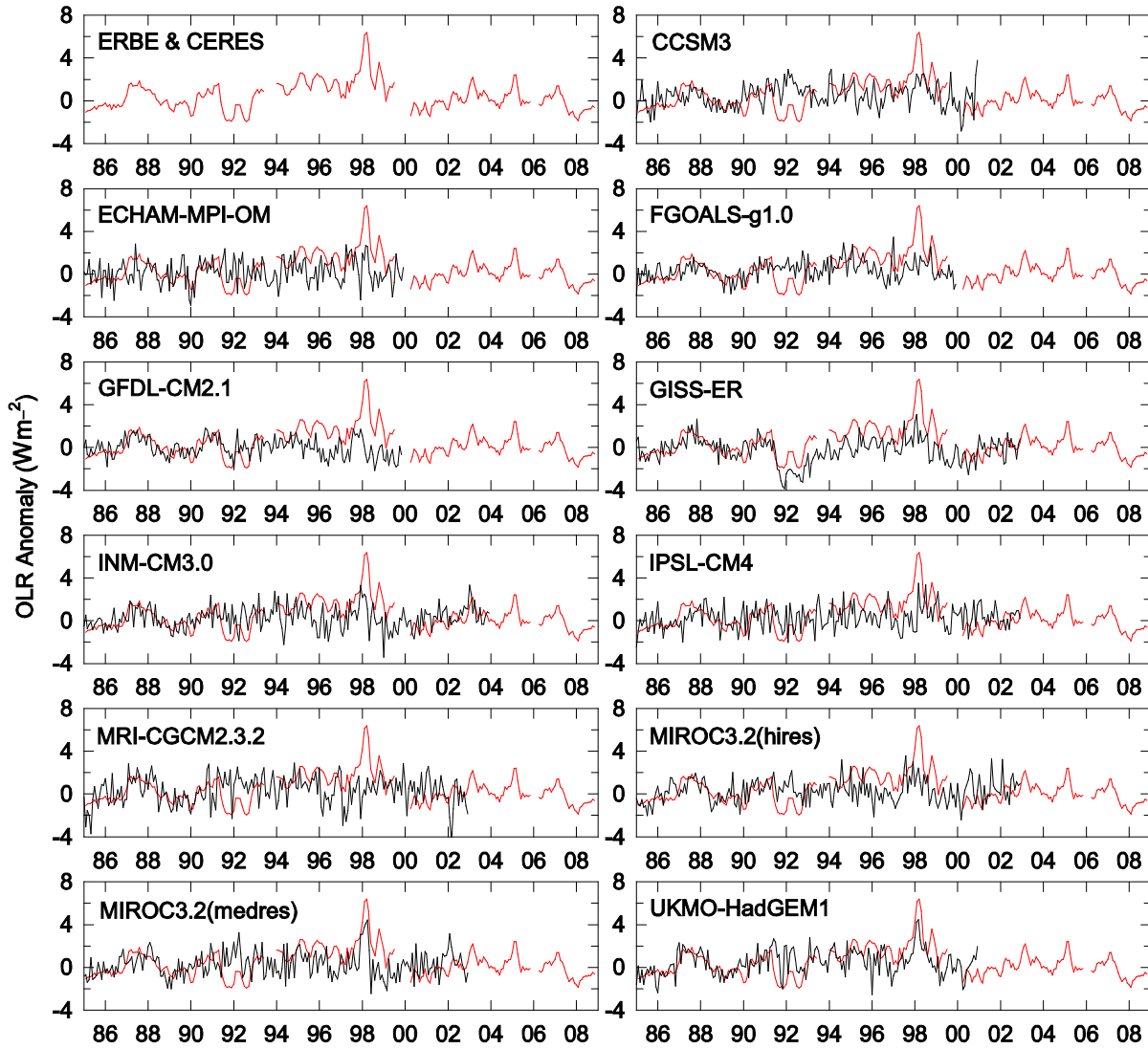
710

711 Figure 4
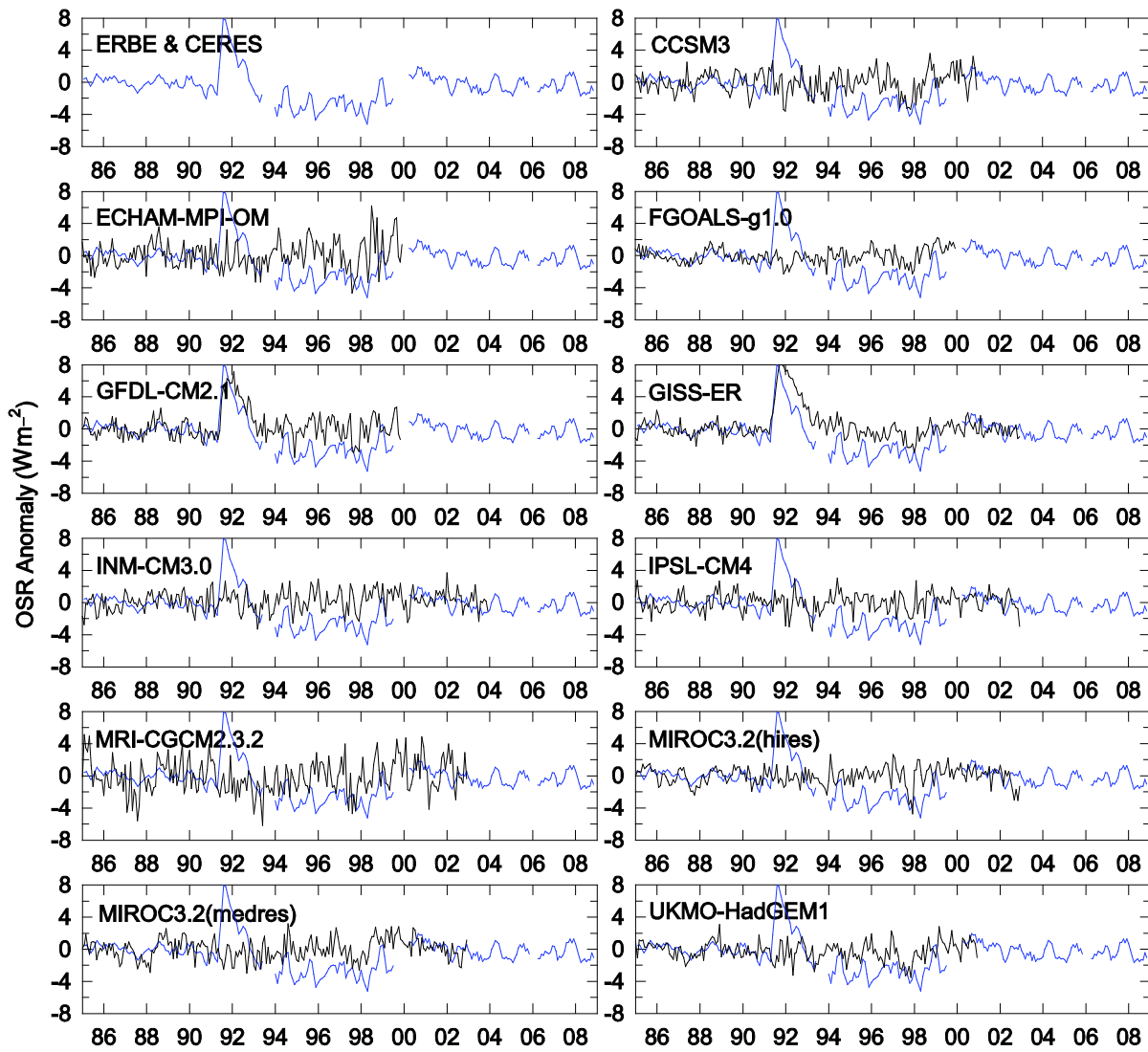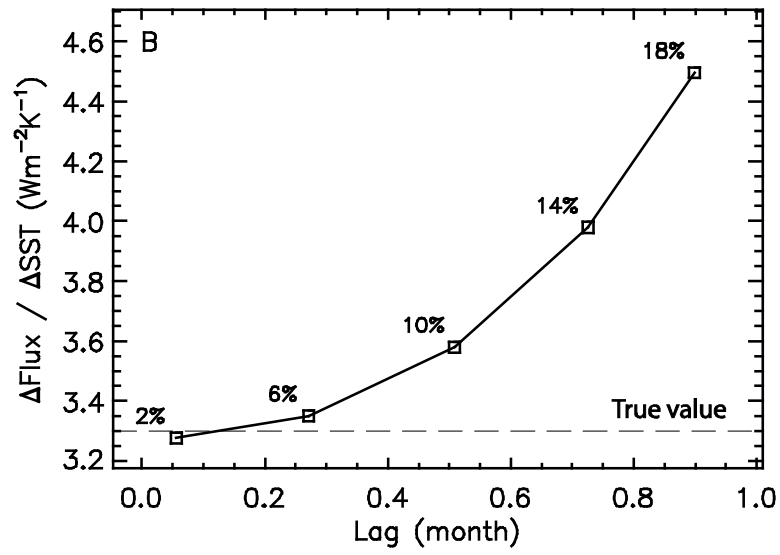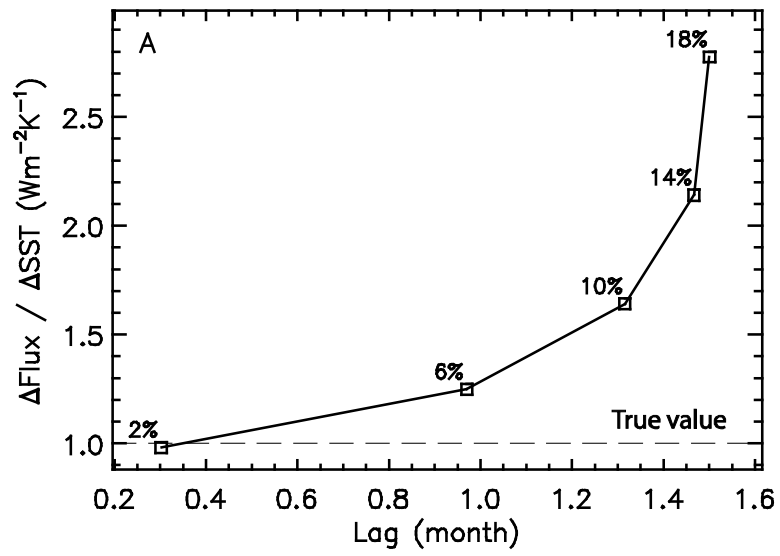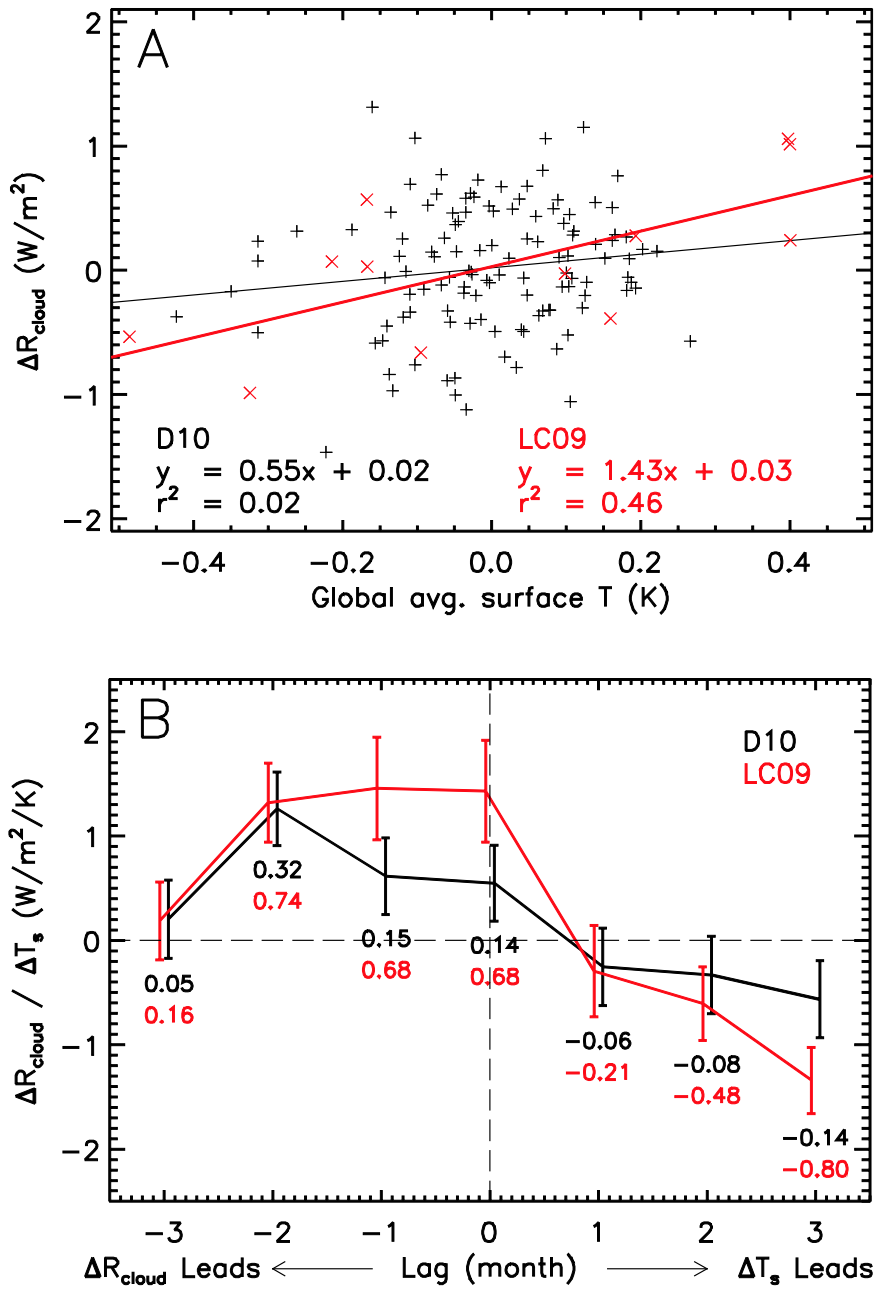
712

713   Figure 5
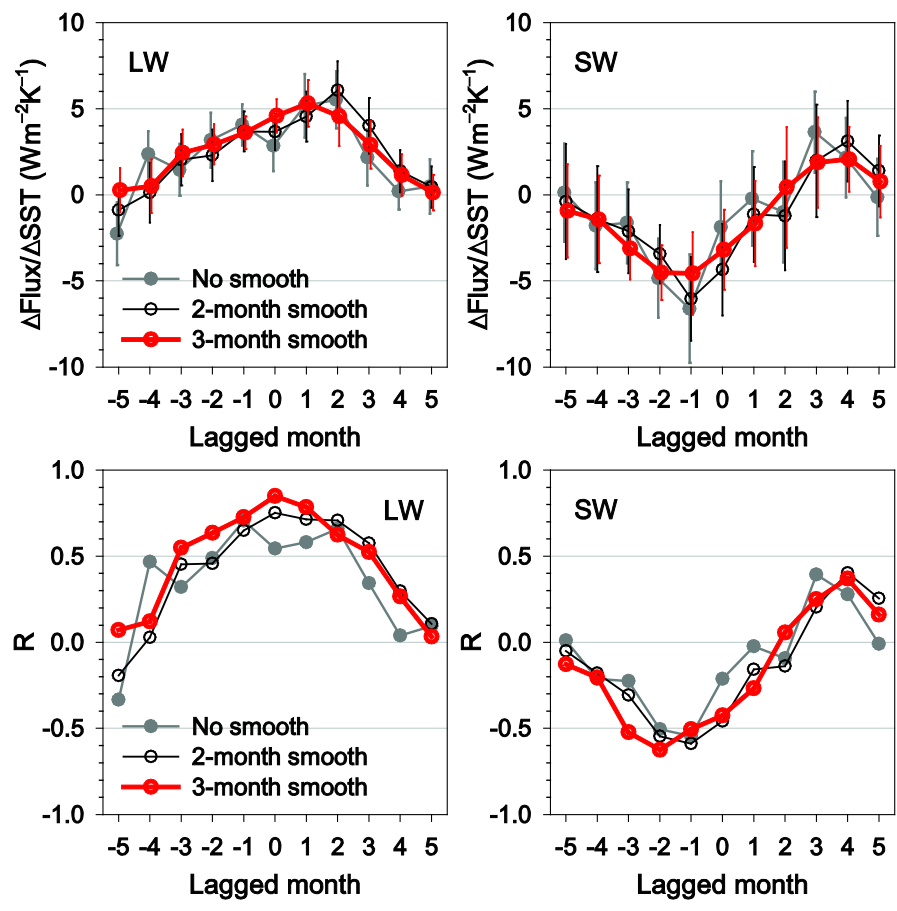
714
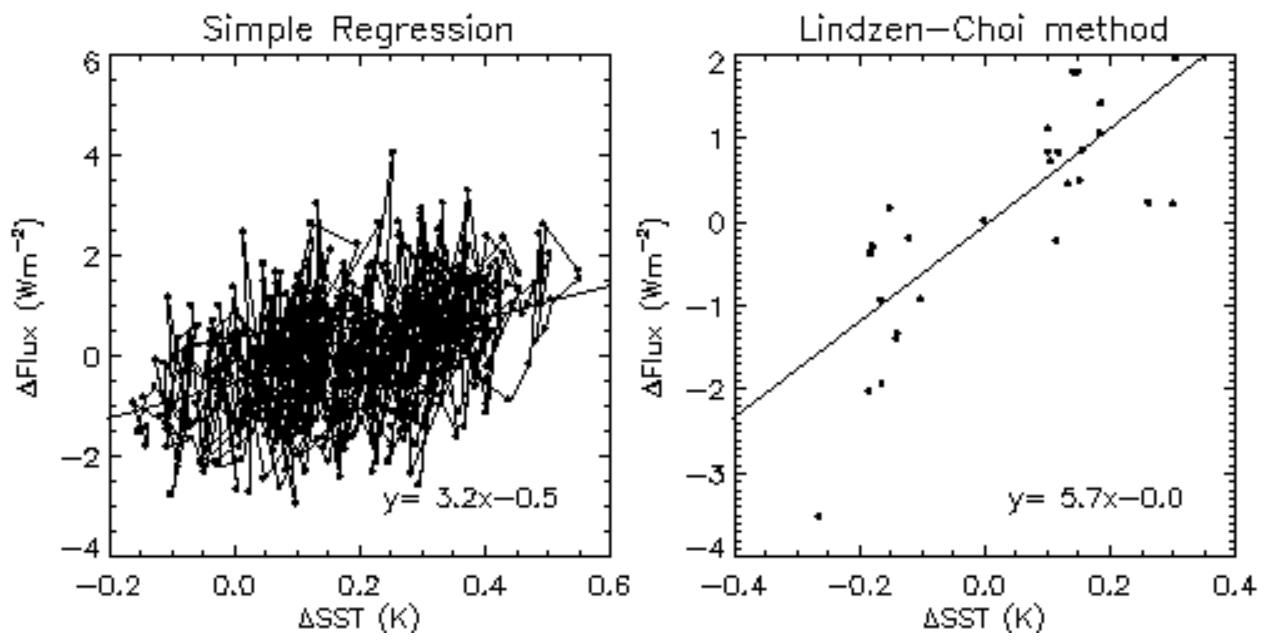
715

716   Figure 6

717
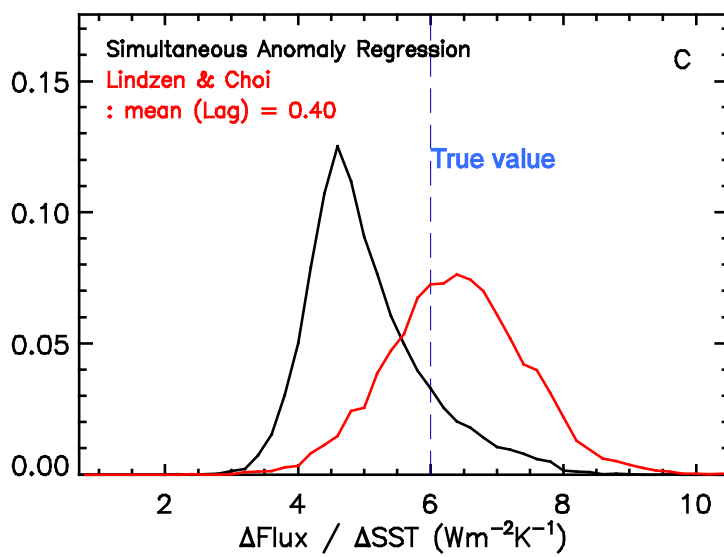
718
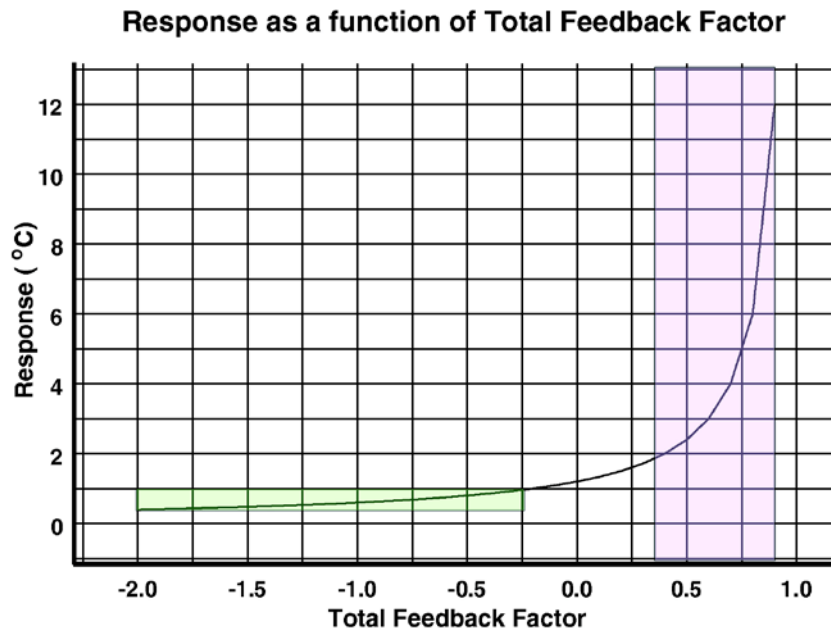
719   Figure 7

720

721

722   Figure 8

723

724

725   Figure 9

728   Figure 10

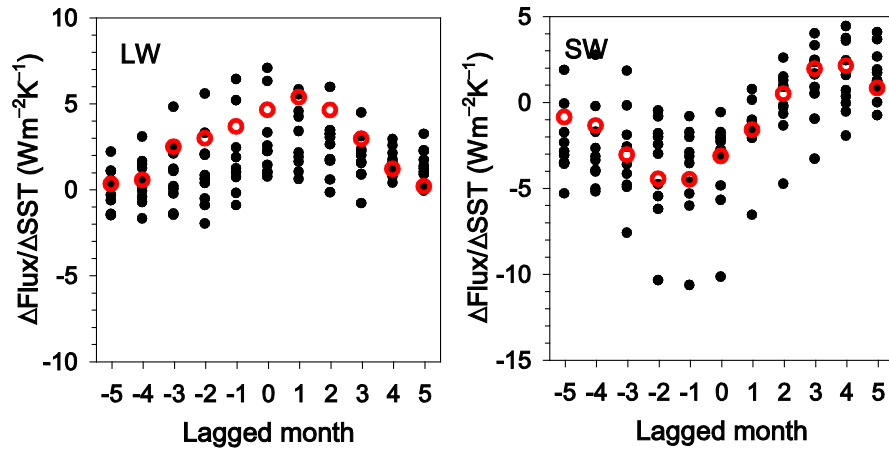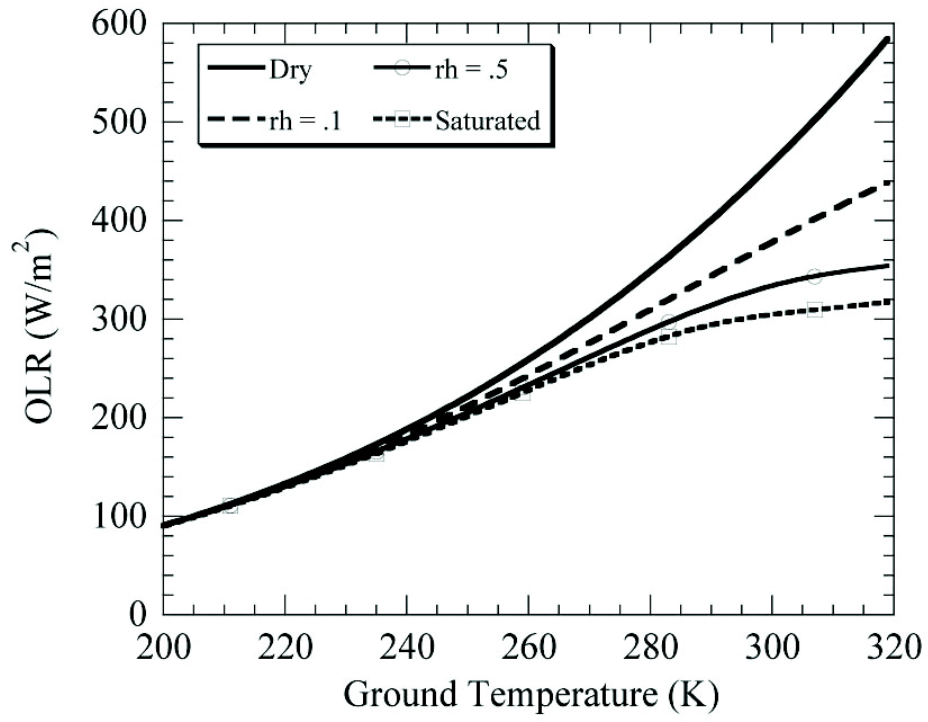**Response as a function of Total Feedback Factor**

730

731   Figure 11

732

733

734   Figure 12

735

736

737   Figure 13

738